LETTER
A Color Restoration Method for Irreversible Thermal Paint Based on Atmospheric Scattering Model

Zhan WANG[†a)], Ping-an DU[†], *Nonmembers, and* Jian LIU[††], *Student Member*

SUMMARY Irreversible thermal paints or temperature sensitive paints are a kind of special temperature sensor which can indicate the temperature grad by judging the color change and is widely used for off-line temperature measurement during aero engine test. Unfortunately, the hot gases flow within the engine during measuring always make the paint color degraded, which means a serious saturation reduction and contrast loss of the paint colors. This phenomenon makes it more difficult to interpret the thermal paint test results. Present contrast enhancement algorithms can significantly increase the image contrast but can't protect the hue feature of the paint images effectively, which always cause color shift. In this paper, we propose a color restoration method for thermal paint image. This method utilizes the atmospheric scattering model to restore the lost contrast and saturation information, so that the hue can be protected and the temperature can be precisely interpreted based on the image.

key words: image processing application, aero-engine, temperature measurement, nondestructive testing, thermal analysis

1. Introduction

Irreversible thermal paints are used by most aeronautical manufacturers in dedicated tests to record temperature profiles over the surface of engine components. These paints can change their colors according to the peak working temperatures and will not change back after it cools down, thus providing an off-line temperature measurement. They can be applied to the large area components or complex surface shapes and do not interfere with the thermal behavior [1].

The thermal paint test process includes two main steps: calibration and implementation. In the calibration step, the paints should be tested on test coupons and heated by an electronic heater to get the performance of each type of paint, which means to get the color-temperature relationship. Then these paints will be applied on engine components and the temperature information will be obtained by comparing the paint colors to the color-temperature relationship [2], [3]. However, in practice, the test condition inside of a running aero engine is much more terrible than an electronic heater. There always be a color degraded in the implementation, which will cause a reduction of saturation
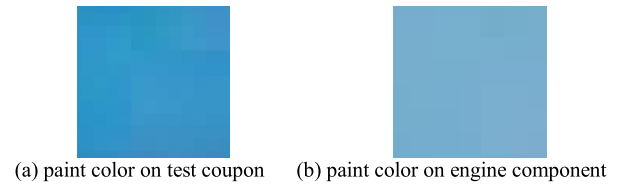
(a) paint color on test coupon   (b) paint color on engine component

Fig. 1 Demonstration of color degrade phenomenon.

and contrast, see Fig. 1. This phenomenon makes the color-temperature matching processing more difficult and affects the accuracy of the interpretation. To avoid this, in this paper, we propose a simple but efficient method to restore the color profile of thermal paint image, which can enhance the color contrast and do not influence the hue. This method includes 2 parts, one for the light source correction, the other for the image enhancement. They will be introduced respectively in the following sections.

2. Light Source Correction

First we need to fix the light condition into the same to reduce the color impact caused by the light source.

Objects will always keep their color even if the wavelength changes or the light source's energy composition changes. This phenomenon is called color constancy and plays an important role in computer vision research. The Retinex theory is an effective light correction solution based on the color constancy. Before the color restoration, we add a process based on the Retinex theory to fix the light condition [4], [5]. The process is explained as follow.

In Retinex theory, the captured image can be defined as:

$$I(x_s) = n_l \cdot n_o \int_\lambda R(\lambda, x_o) L(\lambda) S(\lambda) d\lambda \qquad (1)$$

where $I(x_s)$ is the pixel values of each channel at position x_s in the captured image, n_l and n_o are the unit vector pointing the light source direction and the surface normal respectively, λ is the wavelength, $R(\lambda, x_o)$ represents the light reflect percentage on the Lambertian surface at position x_o, $L(\lambda)$ is the light source intensity, $S(\lambda)$ is the camera's response functions.

In practice, the equation can be simplified as

$$I_i(x_s) = R(\lambda_i, x_o) L(\lambda_i) \qquad (2)$$

where $I_i(x_s)$ represents the ith component of the pixel val-

ues (R,G,B). Then, the color constancy can be achieved by independently scaling the three channels.

For the image acquisition, the test coupons (or engine components) should be set in a standard background. The standard background's color RGB (r1,r2,r3) should be as close as to ideal white RGB (255,255,255), so that it can reflect the light source of each wavelength as much as possible. In this way, the pixel values of the standard background in each channel can represent the top 10% brightest of the whole image. Under an optimum light condition $L_s(\lambda_i)$, the background average color value $I_i(x_{white})$ in the image can be extracted, for example as RGB (221,225,231). Therefore, the reflectance at background surface position x_b is

$$R(\lambda_i, x_b) = \frac{I_i(x_{white})}{L_s(\lambda_i)} \quad (3)$$

When a new image is captured in other light condition $L'(\lambda_i)$, we can estimate the $I'_i(x_{white})$ with the top 10% brightest pixel value in the image (background color). Since the reflectance at the same position is constant, we have

$$\frac{I_i(x_{white})}{L_s(\lambda_i)} = \frac{I'_i(x_{white})}{L'(\lambda_i)} = R(\lambda_i, x_b) \quad (4)$$

The thermal paint images are always captured in close-range, we can assume that light conditions and scene depths are very similar in the whole image. Then all the pixel value under the optimum light condition can be estimated as follow:

$$I_i(x_s) = R(\lambda_i, x_0)L_s(\lambda_i) \quad (5)$$

and

$$R(\lambda_i, x_0) = \frac{I'_i(x_s)}{L'(\lambda_i)} \quad (6)$$

where $I'_i(x_s)$ is the pixel value at position x_s under light condition $L'(\lambda_i)$. According to Eq. (4),

$$L_s(\lambda_i) = \frac{L'(\lambda_i)I_i(x_{white})}{I'_i(x_{white})} \quad (7)$$

Finally, combining Eqs. (5)–(7),

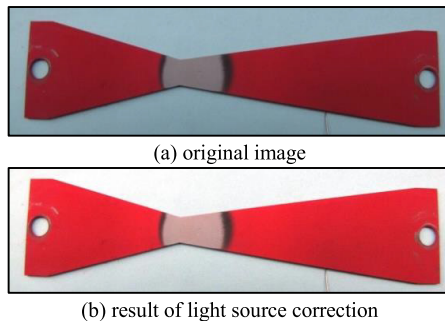$$I_i(x_s) = \frac{I_i(x_{white})I'_i(x_s)}{I'_i(x_{white})} \quad (8)$$

(a) original image

(b) result of light source correction

Fig. 2 Demonstration of light source correction

The effect of the light source correction is demonstrated in Fig. 2.

3. Color Restoration

The purpose of most present contrast enhancement algorithms is to extend the image color to a larger range, which is an effective approach to enhance the nature images. However, different from nature images, the number of colors in each thermal paint image is very limited. If the paint colors are extended to a larger range, it will cause a serious color shift, i.e. the hue value changes, which will badly effects the accuracy of thermal paint interpretation. Therefore, we try to find another way to enhance the thermal paint images.

Figure 3 shows 23 typical thermal paint colors which are captured in the calibration stage. Except the "black" and the "white" (No.1 and No.23), the rest paint colors always have at least one channel which's value is much lower than the other channels.

This phenomenon is similar to the "dark channel prior", which is an effective image prior for the haze removal problem [6]. Therefore, we propose an interesting assumption: if the paint color degrade phenomenon is caused by the atmospheric scattering (haze) [7], then we can use the atmospheric scattering model to restore the color.

The atmospheric scattering model is shown as follow:

$$I(x) = J(x)t(x) + A(1 - t(x)) \quad (9)$$

Where $I(x)$ is the observed RGB color of the pixel at position x, which is color degraded. In this paper, $J(x)$ represents the original thermal paint color, $t(x)$ is the transmission of the reflected light, A is the global atmospheric light. The purpose of our method is to get the $J(x)$, then we have

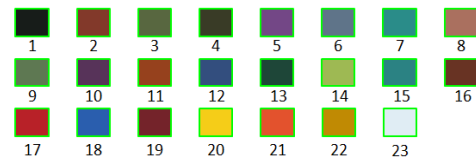$$J(x) = \frac{I(x) - A}{t(x)} + A \quad (10)$$
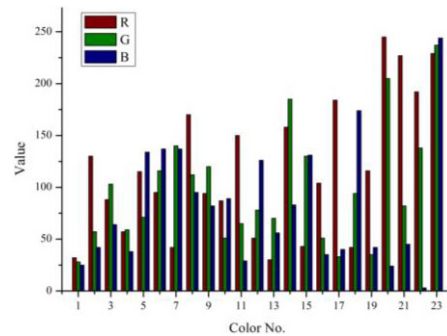

Fig. 3 Thermal paint color

Fig. 4 RGB relationship of paint colors

the $t(\text{x})$ and A are unknown and they can be estimated respectively as follow:

For the $t(\text{x})$, first, normalize the Eq. (9) by A, we have

$$\frac{I^c(\text{x})}{A^c} = t(\text{x})\frac{J^c(\text{x})}{A^c} + 1 - t(\text{x}) \tag{11}$$

where $I^c(\text{x})$ and $J^c(\text{x})$ means each channel of I(x) and J(x). Then, the minimum operators is applied on both sides

$$\min_{y \in \Omega(x)}\left(\min_c \frac{I^c(y)}{A^c}\right) = \tilde{t}(\text{x}) \min_{y \in \Omega(x)}\left(\min_c \frac{J^c(y)}{A^c}\right) + 1 - \tilde{t}(\text{x}) \tag{12}$$

and

$$\min_{y \in \Omega(x)}\left(\min_c \frac{J^c(y)}{A^c}\right) = \frac{J_{low}}{\min_c A^c} = k \tag{13}$$

where J_{low} means the average of the dark channel values in the calibration stage image. The dark channel here represents the channel which has the lowest value. Thus,

$$\tilde{t}(x) = \frac{1 - \omega \min_{y \in \Omega(x)}\left(\min_c \frac{I^c(y)}{A^c}\right)}{1 - k} \tag{14}$$

where parameter ω (range: 0–1) is used to control the enhancement intensity. Based on experience, we fix it as 0.7 to get a better effect.

Now, in Eq. (10), only A is unknown. According to the dark channel prior and the characteristics of thermal paint images, we estimate the A with the top 1% brightest pixels in the dark channel. In these pixels, we pick the pixels which have the highest intensity in I as the A.

4. Implementation and Testing

In this section, the color restoration method is tested on typical thermal paint images and the results are compared with three present image enhancement algorithms: histogram equalization, MSRCR (Multi-Scale Retinex with Color Restore) and adaptive contrast. Two sets of test results are shown in Fig. 5 and Fig. 8 respectively.

The image contrast is compared by the MSE (Mean squared error) contrast [8], which is given by

$$C_{MSE} = \sum_{c \in \{R,G,B\}} \sum_{p=1}^{N} \frac{(J_c(p) - \bar{J}_c)^2}{N} \tag{15}$$

where $J_c(p)$ is the pixel value in each channel, $\bar{J}_c$ is the average of $J_c(p)$ and N is the pixel number in a block. Results show that all the four test methods have good performance in contrast enhancement. Because the MSRCR extends the images' dynamic range, the contrast enhancement is more strong. However, it also breaks the hue of each area.

In Fig. 6 and Fig. 9, the result images are converted into HSI color space (Hue, Saturation, Intensity), and the
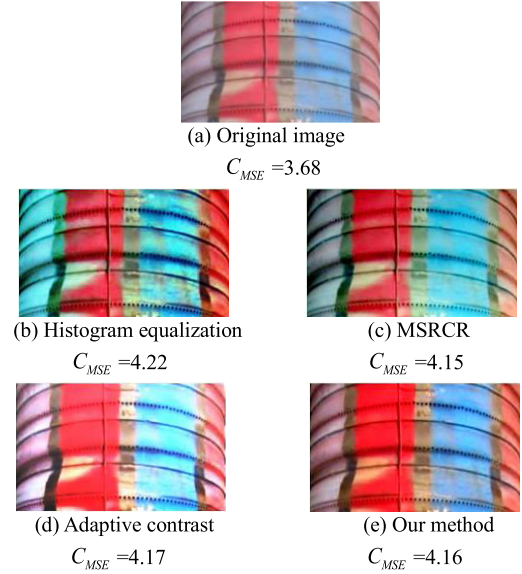

(a) Original image
C_{MSE} =3.68

(b) Histogram equalization
C_{MSE} =4.22

(c) MSRCR
C_{MSE} =4.15

(d) Adaptive contrast
C_{MSE} =4.17

(e) Our method
C_{MSE} =4.16

Fig. 5 Test result 1.

(a) Original image

(b) Our method

(c) Adaptive contrast
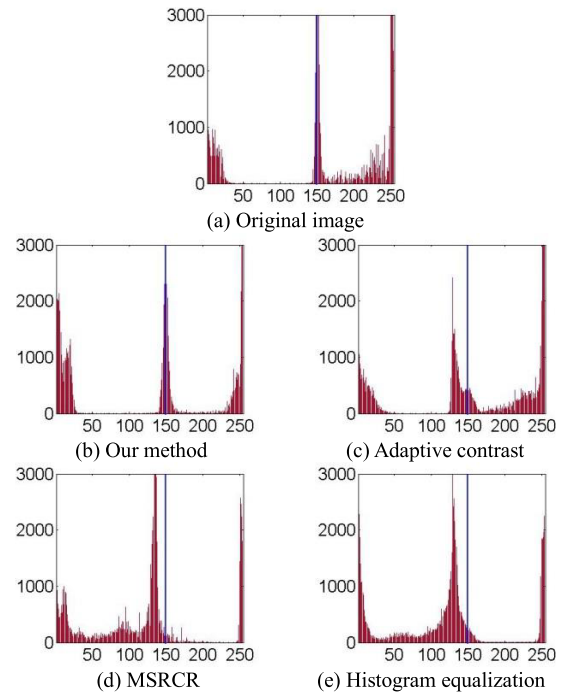
(d) MSRCR

(e) Histogram equalization

Fig. 6 Histogram of hue channel in test 1

hue channel histogram (vertical axis: pixel number, horizontal axis: Hue) is calculated to see if the hue will be affected. The vertical lines indicate the original image histogram peak positions. Results of our method show that the hue peaks have a better agreement with the original image, which means the hue value is well protected. Specifically, in Fig. 6, the peak in the middle of each histogram represents the blue area in Fig. 5. Figure 6 (b) shows that our method effectively protects the peak position. The other peak is at the edge of the histogram, so it's not labeled. In Fig. 9, our method also has better performance in hue protection.
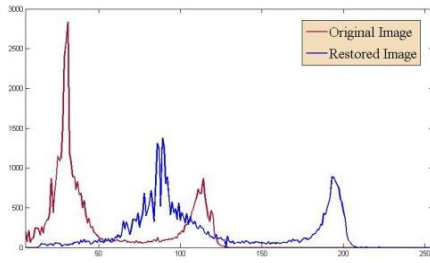
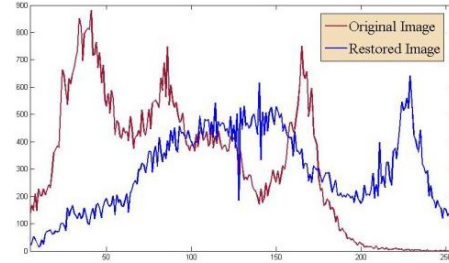**Fig. 7**   Saturation histogram in test 1.

Fig. 10   Saturation histogram in test 2.

Figure 7 and Fig. 10 compare the color saturation histograms of the original image and color restored image in test 1 and test 2 respectively. The results show that after our color restoration processing, the saturation is enhanced effectively.

5.   Conclusion

This research explores the thermal paint color degraded phenomenon. Based on the similarity between the thermal paint color degraded phenomenon and the atmospheric scattering, the paint color restoration problem is transformed into a haze removal problem. By improving the atmospheric scattering model, this letter proposes a color restoration method especially for thermal paint images, which has been proved to have a good effect to assist the thermal paint automatic interpretation.

(a) Original image
C_{MSE} =3.39

(b) Histogram equalization
C_{MSE} =4.12

(c) MSRCR
C_{MSE} =3.81

(d) Adaptive contrast
C_{MSE} =4.09

(e) Our method
C_{MSE} =4.03

Fig. 8   Test result 2.

(a) Original image

(b) Our method

(c) Adaptive contrast

(d) MSRCR

(e) Histogram equalization

Fig. 9   Histogram of hue channel in test 2

References

[1] S.V. Bhalerao, A.N. Pawar, U. Chandrashekhar, and M. Sarode, "Development and application of a universal filter in image processing for automatic interpretation of temperature-sensing thermal paints," Experimental Techniques, vol.38, no.1, pp.38–47, 2014.

[2] C. Lempereur, R. Andral, and J.Y. Prudhomme, "Surface temperature measurement on engine components by means of irreversible thermal coatings," Measurement Science & Technology, vol.19, no.19, p.105501, 2008.

[3] Y. Li and Z.M. Li, "The research of temperature indicating paints and its application in aero-engine temperature measurement," in 2014 asia-pacific international symposium on aerospace technology, pp.1152–1157, 2014.

[4] D.J. Jobson, Z. Rahman, and G.A. Woodell, "A multiscale retinex for bridging the gap between color images and the human observation of scenes," IEEE Trans. Image Process., vol.6, no.7, pp.965–976, 1997.

[5] Z. Rahman, D.J. Jobson, and G.A. Woodell, "Multi-scale retinex for color image enhancement," International Conference on Image Processing, 1996. Proceedings, vol.1003, pp.1003–1006, 2002.

[6] K. He, J. Sun, and X. Tang, "Single image haze removal using dark channel prior," 2009 IEEE Conference on Computer Vision and Pattern Recognition, pp.1956–1963, 2009.

[7] S.G. Narasimhan and S.K. Nayar, "Vision and the atmosphere," International Journal of Computer Vision, vol.48, no.3, pp.233–254, 2002.

[8] J.-H. Kim, W.-D. Jang, J.-Y. Sim, and C.-S. Kim, "Optimized contrast enhancement for real-time image and video dehazing," Journal of Visual Communication & Image Represen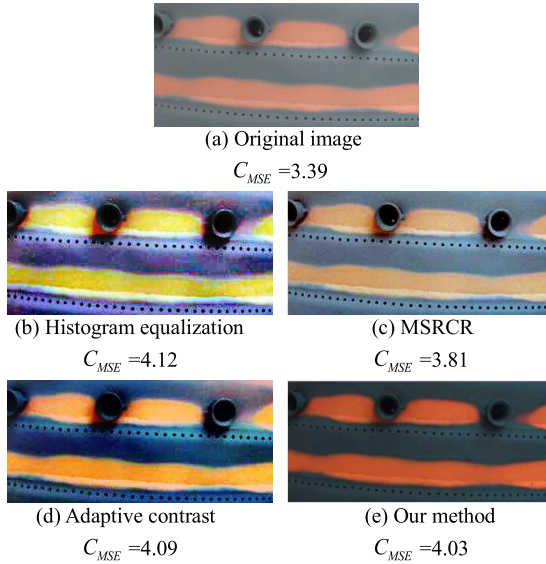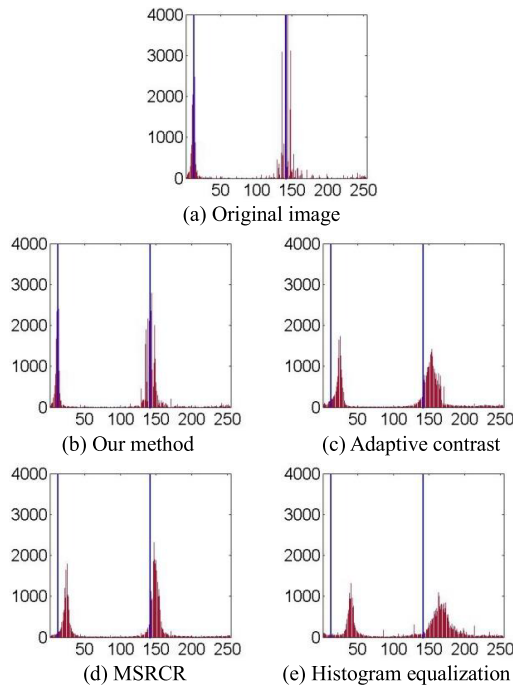tation, vol.24, no.3, pp.410–425, 2013.